

Above-barrier resonances: analytical expressions for energy and width

This article has been downloaded from IOPscience. Please scroll down to see the full text article.

2002 J. Phys. A: Math. Gen. 35 4349

(<http://iopscience.iop.org/0305-4470/35/19/314>)

View [the table of contents for this issue](#), or go to the [journal homepage](#) for more

Download details:

IP Address: 171.66.16.106

The article was downloaded on 02/06/2010 at 10:04

Please note that [terms and conditions apply](#).

# Above-barrier resonances: analytical expressions for energy and width

B Sahu<sup>1</sup>, S K Agarwalla<sup>1</sup> and C S Shastry<sup>1,2</sup>

<sup>1</sup> Department of Physics, Khallikote College, Berhampur-760 001, India

<sup>2</sup> Department of Physics, North Eastern Hill University, Shillong, India

Received 5 March 2002

Published 3 May 2002

Online at [stacks.iop.org/JPhysA/35/4349](http://stacks.iop.org/JPhysA/35/4349)

## Abstract

We construct a smooth realistic barrier potential that can generate resonances above the top of the barrier provided a parameter  $\lambda$  controlling the flatness of the barrier is larger than the critical value  $\lambda = \sqrt{2}$ . The energies and widths of resonances are expressed analytically in terms of the characteristics of the barrier, namely height, range and flatness. In order to obtain a more versatile and asymmetric barrier, two symmetric barriers are merged together side by side and the exact transmission coefficient across such a barrier is derived.

PACS numbers: 11.30.Pb, 11.55.–m

## 1. Introduction

The characterization of resonances and their role in the behaviour of the scattering amplitude is an important topic in the theory of potential scattering. In the  $S$ -matrix theory, the bound states and resonances associated with a particle moving under a potential,  $V(r)$ , are represented in terms of poles of the  $S$ -matrix in the complex momentum ( $k$ -) plane [1]. The bound-state poles are known to occur on the positive imaginary  $k$ -axis, giving a negative-energy state. The resonance poles represent decaying states with positive energy  $E^R$  and width  $\Gamma$ . One expects that sharp resonances will occur when the potential function has a pocket capable of trapping the particle to generate a long-lived state, and its decay is due to tunnelling away from the pocket to infinity. It may be noted that in the classical situation particles trapped in such potential pockets will generate bound orbits.

In the process of collision of two heavy nuclei, the occurrence of resonances is an important phenomenon [2]. The general feature of the heavy-ion potential including the Coulomb interaction and the centrifugal term ( $\frac{\hbar^2}{2m} \frac{l(l+1)}{r^2}$ ,  $l > 0$ ) shows a potential pocket in the interior region and a large Coulomb barrier on the surface region. Heavy-ion collision is characterized by strong absorption in the interior and, hence, the resonance states that may be generated by the pocket will have large widths. Therefore, one examines the possibility of occurrence of resonances due to an orbiting-like phenomenon in the barrier region [3–7]. The barrier

top is a point of unstable equilibrium. The question arises of whether a potential barrier can generate quantal resonance states at energies above the top of it which can be termed as above-barrier resonances (ABRs). The answer to this question is in the affirmative in the case of a rectangular barrier, where discrete resonances are observed above the top of the barrier. However, in the case of a realistic smooth barrier, the occurrence of ABRs is not clearly visualized and formulated in terms of the characteristics of the barrier. In this context, we note below some well known analytically solvable smooth barrier potentials, namely parabolic, Eckart and Morse, and point out their inability to produce observable ABRs.

Friedman and Goebel in their paper [6] have obtained the following expression for the barrier top resonance pole in the complex energy plane for different partial waves  $l$ :

$$E_{n,l} = V_0 - i(2n + l + 3/2)\omega, \quad n = 0, 1, 2, \dots \quad (1)$$

in the case of a spherically symmetric parabolic potential barrier

$$V(r) = V_0 - \frac{1}{2}m\omega^2 r^2, \quad r \geq 0. \quad (2)$$

Here,  $V_0$  and  $\omega$  indicate the height and oscillator frequency of the barrier, respectively. We note that equation (1) essentially manifests a kind of *degeneracy*. That is, at the same real energy we have an accumulation of infinitely many levels of steadily increasing widths. The question arises of whether this can manifest an observable sharp resonance. For example, equation (1) indicates the situation when a large number of broader resonances ( $n = 1, 2, 3, \dots$ ) are superposed on the sharpest resonance, corresponding to  $n = 0$ , for a particular  $l$ . As a consequence one has a situation in which no resonance character is observed at the top of the barrier.

Let us consider another example of an exactly solvable smooth barrier. This is the general Eckart potential barrier given by [8]

$$V(x) = -\frac{A\xi}{1-\xi} - \frac{B\xi}{(1-\xi)^2}, \quad (3)$$

where  $\xi = -e^{2\pi x/a}$ ,  $A$  and  $B$  are constants and  $a$  represents the slope of the barrier potential. This can generate an asymmetric barrier with long-range character on one side. If  $A = 0$ , a symmetric potential is obtained with

$$V(x) = (B/4)\operatorname{sech}^2\left(\frac{\pi x}{a}\right) \quad (4)$$

which possesses a maximum of  $\frac{B}{4}$  at  $x = 0$ . As clearly shown in [8], this potential barrier in either symmetric or asymmetric form cannot generate any resonance at energy above the barrier.

The Morse barrier potential expressed as

$$V(x) = B[2e^{(x/a)} - e^{(2x/a)}], \quad (5)$$

where  $B$  and  $a$  indicate the height and slope of the barrier, respectively, is another idealization of smooth potential barriers which is analytically solvable for transmission coefficient etc. It can be clearly seen from the exact expression for transmission amplitude [9] that discrete resonances can never be produced in the above-barrier region of energy.

In view of the above observations, it is highly essential to search for a potential barrier which can generate discrete ABRs and at the same time the barrier is smooth, short ranged, ideal and analytically solvable for wider applicability in physical processes.

In this paper, we construct a barrier potential by modifying an attractive one-dimensional potential expressed by Ginocchio in [10]. This barrier is found to be smooth, symmetric, flat at the top, maximum at  $x = 0$  and short ranged due to convergence on both sides ( $x \rightarrow \pm\infty$ ).

Having obeyed a condition on the flatness of the barrier, this barrier can generate discrete ABRs in which the sharpest resonance is found close to the barrier top. As the potential is exactly solvable, the energy and width of the ABRs are expressed analytically in terms of the characteristics of the barrier, namely height, range and flatness. The parameter  $\lambda$  controlling the flatness of the barrier is such that if  $\lambda > \sqrt{2}$ , ABR occurs. Interestingly, when  $\lambda = 1$ , this potential barrier reduces to the symmetric form of the Eckart potential given by equation (4), which fails to generate any ABR.

Our study in this paper is restricted to one dimension. However, the condition and conclusion on ABR stated above can be shown to be valid in the three-dimensional situation also by considering the potential expressed by Ginocchio in [11].

Further, in order to generate an asymmetric nature in the barrier having unequal slopes or ranges on either side of it, two symmetric potential barriers as considered above are merged together side by side. The transmission coefficient across such a composite barrier is expressed analytically. Such a technique of merging has been performed in [12, 13] but the potentials considered are infinite ranged inverted harmonic oscillators of the type given by (2), which tend to  $-\infty$  as  $x \rightarrow \pm\infty$  and cannot produce ABR. Our present merged potential barrier, which converges on both sides, incorporates both aspects: asymmetry and ABR. Hence, it is more versatile and realistic. As the Coulomb barrier in nucleus–nucleus potential is found to be generally asymmetric, smooth and practically short ranged in nature and resonance is an important event occurring in the collision process, the exact expression for the transmission coefficient across such an asymmetric barrier which can generate ABR as well may be more suitable for the analysis of measured data of fusion in the collision of two nuclei at low energies. However, earlier, we used, in such an analysis [14], the expression for transmission coefficient across the merged parabolic barrier [12] with limited success.

In section 2, we develop the symmetric barrier and obtain the expressions for transmission coefficient, resonance energy and width. In section 3, the merging of two symmetric barriers is carried out and the expression for transmission coefficient is derived. Section 4 contains the discussion and conclusion.

## 2. The symmetric potential barrier

We modify the one-dimensional attractive potential given by Ginocchio [10] and obtain and analyse a symmetric barrier potential as follows.

In the Schrödinger equation

$$\left[ -\frac{\hbar^2}{2m} \frac{d^2}{dx^2} + V(x) \right] \psi(x) = E\psi(x), \quad (6)$$

the potential  $V(x)$  is expressed in the form

$$V(x) = V_0 v(bx), \quad (7)$$

where  $V_0$  represents the strength of the potential in units of energy and  $b$  is the scale parameter in units of inverse distance given by

$$b = \left( \frac{2m}{\hbar^2} V_0 \right)^{1/2}. \quad (8)$$

Here,  $m$  denotes the mass of the particle moving under the potential  $V(x)$ .

Using the dimensionless distance variable  $r = bx$ , we write the functional form  $v(r)$  of the potential

$$v(r) = \lambda^2 v(v+1)(1-y^2) + \frac{1-\lambda^2}{4} [5(1-\lambda^2)y^4 - (7-\lambda^2)y^2 + 2](1-y^2). \quad (9)$$

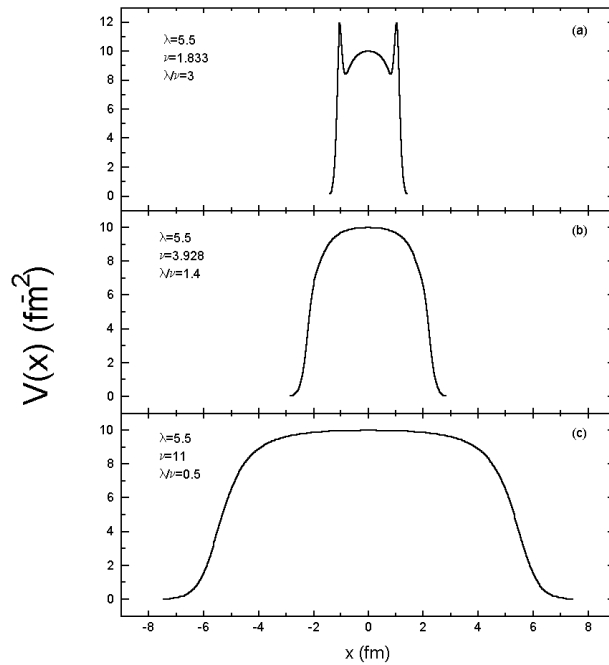


**Figure 1.** Plot of potential as a function of distance. The height of the barrier  $V_B = V_0[\lambda^2(\nu^2 + \nu - \frac{1}{2}) + \frac{1}{2}]$  at the origin is equated to  $10 \text{ fm}^{-2}$ . In all three cases,  $\lambda = 5.5$  but  $\nu$  is different: (a)  $\nu = 1.833$  and  $\frac{\lambda}{\nu} = 3$ , (b)  $\nu = 3.9286$  and  $\frac{\lambda}{\nu} = 1.4$ , (c)  $\nu = 11$  and  $\frac{\lambda}{\nu} = 0.5$ .

Here,  $\lambda$  and  $\nu$  are two dimensionless parameters. The parameter  $\nu$  measures the height of the barrier. The parameter  $\lambda$  accounts for the shape of the barrier. The function  $y(r)$  is related to the radial variable  $r$  by

$$r = \frac{1}{\lambda^2} [\tanh^{-1} y - (1 - \lambda^2)^{1/2} \tanh^{-1} (1 - \lambda^2)^{1/2} y]. \quad (10)$$

While the range of  $r$  is  $-\infty \leq r \leq \infty$ , the range of  $y$  is  $-1 \leq y \leq 1$ . The parameter  $\lambda$  can take any positive value  $0 < \lambda < \infty$ . It may be pointed out here that expression (9) representing a barrier is not just the total negative of the expression for the attractive case considered in [10]. The height of the barrier potential (7) is maximum at the origin  $x = 0$  and is of value

$$V_B = V_0[\lambda^2(\nu^2 + \nu - \frac{1}{2}) + \frac{1}{2}], \quad (11)$$

and it converges symmetrically on both sides as  $x \rightarrow \pm\infty$ . For a fixed value of  $V_B$ , the variation of  $\nu$  will indicate the change in the range of the barrier instead of height. This is exhibited in figure 1 for a typical barrier of height  $V_B = 10 \text{ fm}^{-2}$ . Here, we have considered  $\hbar = 2m = 1$  and expressed energy in  $\text{fm}^{-2}$  units and distance in fm units for convenience. For  $\lambda = 1$ , the potential (7) with (9) reduces to the well known symmetric form of the Eckart potential barrier given by (4) with maximum height at  $x = 0$  equal to  $V_B = B/4 = V_0\nu(\nu + 1)$  and slope parameter  $a = \pi/b$ , where  $b$  is given by (8). For  $\lambda > 1$ , the top of the barrier becomes flatter.

### 2.1. Transmission coefficient

The Schrödinger equation (6) can be written in dimensionless form

$$\left[ -\frac{d^2}{dr^2} + v(r) \right] \Psi(r) = E' \Psi(r), \quad (12)$$

where  $E' = E/V_0$ . Using expression (9) for  $v(r)$ , the above equation can be reduced to Gegenbauer's equation as done in [10]. Finally we obtain the following analytical expression for the wavefunction:

$$\Psi(r) = NG[\lambda^2 + (1 - \lambda^2)z^2]^{1/4} (1 - z^2)^{-\frac{ik}{2\lambda^2}} F\left(\bar{\nu} + 1 - \frac{ik}{\lambda^2}, -\bar{\nu} - \frac{ik}{\lambda^2}, 1 - \frac{ik}{\lambda^2}, \frac{1 - z}{2}\right), \quad (13)$$

where

$$G = \frac{\Gamma(-\bar{\nu} - \frac{ik}{\lambda^2})}{\Gamma(1 - \frac{2ik}{\lambda^2})\Gamma(-\bar{\nu} + \frac{ik}{\lambda^2})}, \quad (14)$$

$$\bar{\nu} = \left[ \frac{1}{4} - \nu(\nu + 1) + \frac{\lambda^2 - 1}{\lambda^4} k^2 \right]^{1/2} - \frac{1}{2}, \quad (15)$$

$$k = |E'|^{1/2} = \sqrt{\frac{E}{V_0}}. \quad (16)$$

Here  $N$  indicates the normalization constant and the last term (function  $F$ ) in expression (13) is the hypergeometric function with variable

$$z = \frac{\lambda y}{[1 + (\lambda^2 - 1)y^2]^{1/2}}. \quad (17)$$

Clearly the range of variation of  $z$  is same as  $y$ . Using the nature of the above wavefunction (13) at  $r = \pm\infty$  and the appropriate boundary condition on either side of the barrier, it is straightforward to arrive at the following expression for the transmission amplitude  $T(E)$  across the barrier:

$$T(E) = \frac{\Gamma(\bar{\nu} + 1 - \frac{ik}{\lambda^2})\Gamma(-\bar{\nu} - \frac{ik}{\lambda^2})}{\Gamma(1 - \frac{ik}{\lambda^2})\Gamma(-\frac{ik}{\lambda^2})} e^{2ikr_1}, \quad (18)$$

where

$$r_1 = \frac{1}{\lambda^2} \log \lambda - r_0,$$

$$r_0 = \frac{(\lambda^2 - 1)^{1/2}}{\lambda^2} \tan^{-1}(\lambda^2 - 1)^{1/2}.$$

The square modulus of expression (18) gives us the transmission coefficient  $T_c$  as

$$T_c(E) = \frac{\cosh(\frac{2\pi k}{\lambda^2}) - 1}{\cosh(\frac{2\pi k}{\lambda^2}) + \cos(2\pi\omega)}, \quad (19)$$

where  $\omega = \left[ \frac{1}{4} - \nu(\nu + 1) + \frac{\lambda^2 - 1}{\lambda^4} k^2 \right]^{1/2}$ , and  $k$  is given by (16).

It is clearly seen that for  $\lambda = 1$  expression (19) reduces to the well known expression for transmission coefficient corresponding to a symmetric Eckart barrier similar to the form of expression (4).

## 2.2. Energy and width of ABR

The resonances generated by the potential barrier can be readily obtained from the position of the maxima of the transmission coefficient  $T_c$  in its variation with energy. Hence, in the corresponding amplitude expression (18), the condition

$$-\bar{v} - \frac{ik}{\lambda^2} = -n, \quad n = 0, 1, 2, \dots$$

leads to the following expressions for resonance energy  $E_n$  and its width  $\Gamma_n$  in terms of the barrier parameters  $v$ ,  $\lambda$  and  $V_0$ :

$$E_n = V_0[(\lambda^2 - 2)(n + \frac{1}{2})^2 + \lambda^2(v^2 + v - \frac{1}{4})], \quad (20)$$

$$\Gamma_n = 4V_0(n + \frac{1}{2})[(\lambda^2 - 1)(n + \frac{1}{2})^2 + \lambda^2(v^2 + v - \frac{1}{4})]^{1/2}. \quad (21)$$

It is clear from (20) that if  $\lambda^2 = 2$  all the resonances ( $n = 0, 1, 2, 3, \dots$ ) are situated at the top of the barrier having the same energy  $E_n = V_B = 2V_0[v^2 + v - \frac{1}{4}]$  as given by equation (11), but when  $\lambda^2 > 2$  we find discrete ABRs starting from the lowest one  $n = 0$  with  $E_0$  close to the top. The corresponding width obtained from expression (21) increases for higher ABRs while  $n = 0$  corresponds to the sharpest resonance. It may be pointed out here that the discrete energies obtained from (20) for  $\lambda^2 < 2$  are all situated below the corresponding maximum height of the barrier and they do not correspond to genuine resonances. Some more discussions on the nature and manifestation of ABRs are given in section 4 below.

## 3. Transmission across a merged composite barrier

We construct here a composite potential barrier by placing side by side two symmetric potentials of the form (9) presented in the previous section. This potential can be expressed as

$$V(x) = V_{01}v_1(r)\theta(-r) + V_{02}v_2(r)\theta(r), \quad (22)$$

where the two step functions have the property  $\theta(r \leq 0) = 0$  and  $\theta(r > 0) = 1$ . Further,

$$v_1(r) = \lambda_1^2 v_1(v_1 + 1)(1 - y^2) + \frac{1 - \lambda_1^2}{4} [5(1 - \lambda_1^2)y^4 - (7 - \lambda_1^2)y^2 + 2](1 - y^2), \quad (23)$$

$$v_2(r) = \lambda_2^2 v_2(v_2 + 1)(1 - y^2) + \frac{1 - \lambda_2^2}{4} [5(1 - \lambda_2^2)y^4 - (7 - \lambda_2^2)y^2 + 2](1 - y^2). \quad (24)$$

Hence, in the region  $r > 0$ , we have  $V(r) = V_{02}v_2(r)$  and in the region  $r \leq 0$ ,  $V(r) = V_{01}v_1(r)$  and  $r$  is the dimensionless distance variable expressed as  $r = b_i x$  with  $b_i = (\frac{2m}{\hbar^2} V_{0i})^{1/2}$ ,  $i = 1, 2$ . The parameters  $v_1, v_2, \lambda_1, \lambda_2$  are dimensionless. Thus, expression (22) represents a composite barrier potential with six parameters  $v_1, v_2, \lambda_1, \lambda_2, V_{01}$  and  $V_{02}$ . By equating the heights of the two side barriers in this expression we obtain a single barrier specified by different sets of parameters on either side. This composite barrier can become symmetric, asymmetric, flatter or less flat on either side depending on the values of the above parameters.

As in the symmetric case, we obtain the exact solutions for the repulsive potentials in the regions  $r < 0$  and  $r > 0$  on either side of the barrier. By using appropriate boundary conditions on these solutions we arrive at the following expression for the transmission coefficient:

$$T_c(E) = \frac{1}{\pi^2} \frac{\lambda_1^3 k_2}{\lambda_2 k_1} \frac{|L_1|^2 |L_2|^2}{|\Gamma(-\frac{ik_1}{\lambda_1})|^2 |\Gamma(1 - \frac{ik_2}{\lambda_2})|^2 |L_2 \lambda_1 + L_1 \lambda_2|^2}, \quad (25)$$

where

$$L_1 = \Gamma\left(\frac{\bar{v}_2}{2} - \frac{ik_2}{2\lambda_2^2} + 1\right) \Gamma\left(-\frac{\bar{v}_2}{2} - \frac{ik_2}{2\lambda_2^2} + \frac{1}{2}\right) \Gamma\left(\frac{\bar{v}_1}{2} - \frac{ik_1}{2\lambda_1^2} + \frac{1}{2}\right) \Gamma\left(-\frac{\bar{v}_1}{2} - \frac{ik_1}{2\lambda_1^2}\right), \quad (26)$$

$$L_2 = \Gamma\left(\frac{\bar{v}_1}{2} - \frac{ik_1}{2\lambda_1^2} + 1\right)\Gamma\left(-\frac{\bar{v}_1}{2} - \frac{ik_1}{2\lambda_1^2} + \frac{1}{2}\right)\Gamma\left(\frac{\bar{v}_2}{2} - \frac{ik_2}{2\lambda_2^2} + \frac{1}{2}\right)\Gamma\left(-\frac{\bar{v}_2}{2} - \frac{ik_2}{2\lambda_2^2}\right), \quad (27)$$

$$\bar{v}_1 = \left[\frac{1}{4} - \nu_1(\nu_1 + 1) + \frac{\lambda_1^2 - 1}{\lambda_1^4}k_1^2\right]^{1/2} - \frac{1}{2}, \quad (28)$$

$$\bar{v}_2 = \left[\frac{1}{4} - \nu_2(\nu_2 + 1) + \frac{\lambda_2^2 - 1}{\lambda_2^4}k_2^2\right]^{1/2} - \frac{1}{2}, \quad (29)$$

$$k_1 = \sqrt{\frac{E}{V_{01}}} \quad \text{and} \quad k_2 = \sqrt{\frac{E}{V_{02}}}.$$

On further simplification, we have

$$T_c(E) = \frac{16\pi^4\lambda_1\lambda_2h_1h_2}{(\lambda_2^2|L_1|^2 + \lambda_1^2|L_2|^2)(s_1^2 + h_1^2)(s_2^2 + h_2^2) + 8\pi^4\lambda_1\lambda_2(s_1s_2 + h_1h_2)}, \quad (30)$$

where  $s_1 = \sin(\pi\bar{v}_1)$ ,  $s_2 = \sin(\pi\bar{v}_2)$ ,  $h_1 = \sinh(\frac{\pi k_1}{\lambda_1^2})$  and  $h_2 = \sinh(\frac{\pi k_2}{\lambda_2^2})$ .

Clearly, when  $\lambda_1 = \lambda_2 = \lambda$ ,  $\nu_1 = \nu_2 = \nu$  and  $V_{01} = V_{02} = V_0$  we get back the transmission coefficient (19) for the symmetric case.

#### 4. Discussion and conclusion

As pointed out in the introduction, an Eckart barrier, symmetric or asymmetric, does not generate any ABR. This result of no resonance in the symmetric case is quite clearly seen in our present formulation (20) when  $\lambda = 1$  corresponding to the symmetric Eckart potential. Now, in order to confirm the result of the asymmetric situation, we consider expression (25) of  $T_c$  corresponding to the merged barrier potential given by (22). Using  $\nu_1 \neq \nu_2$  and  $\lambda = 1$ , we can compute (25) and find that no resonances can be generated in this asymmetric but smooth barrier as in the symmetric Eckart barrier potential.

Choosing different values for  $\nu_1$ ,  $\nu_2$ ,  $\lambda_1$  and  $\lambda_2$  we can generate a variety of potential barriers with different flatness and range on either side of the barrier. All these barriers will be generating ABR provided they satisfy the condition  $\lambda_i^2 > 2$ ,  $i = 1, 2$ .

In order to illustrate some interesting features of ABR, we consider, in the symmetric situation, the maximum height of the barrier given by (11) fixed at  $V_B = 10 \text{ fm}^{-2}$  and change the values of  $\lambda$  and  $\nu$  to generate different barriers. Taking  $\lambda = 5.5$  and using different values of  $\nu$  we see that if the ratio  $\frac{\lambda}{\nu} < 1.4$  there is always a single barrier. On the other hand, if  $\frac{\lambda}{\nu} > 1.4$ , the single barrier starts to become a double barrier with a pocket in the middle. This is also true for other values of  $\lambda$ . In figure 1, we show such potential barriers with three different sets of parameters: (a)  $V_B = 10 \text{ fm}^{-2}$ ,  $\lambda = 5.5$ ,  $\frac{\lambda}{\nu} = 3$ , (b)  $V_B = 10 \text{ fm}^{-2}$ ,  $\lambda = 5.5$ ,  $\frac{\lambda}{\nu} = 1.4$ , and (c)  $V_B = 10 \text{ fm}^{-2}$ ,  $\lambda = 5.5$ ,  $\frac{\lambda}{\nu} = 0.5$ . It is seen that a larger value of  $\nu$  generates a long-ranged potential as shown in figure 1(c). Fixing the height of the barrier at the origin at  $10 \text{ fm}^{-2}$  and taking the value of  $\lambda = 5.5$ , we compute the results of resonance energy  $E_n$  and width  $\Gamma_n$  by using equations (20) and (21), respectively, as functions of the range parameter  $\nu$ . These are plotted in figure 2 for the first three states,  $n = 0, 1$  and  $2$ . It is clearly seen that when  $\nu$  is large the resonances (upper panel) are found close to the top of the barrier ( $V_B = 10 \text{ fm}^{-2}$ ) and they are sharper (small  $\Gamma_n$ ) (lower panel) than those for smaller  $\nu$ .

Besides generation of a large number of resonances with smaller widths, the manifestation of resonances in physically observable quantities, namely cross section and, hence, transmission coefficient, is an important aspect. In this respect, the spacing between adjacent levels  $\Delta E_n = E_{n+1} - E_n$  obtained from expression (20) for the resonance energy should be compared with the width  $\Gamma_n$  given by equation (21) of the  $n$ th level. If  $\Delta E_n \geq \Gamma_n$ , then one can



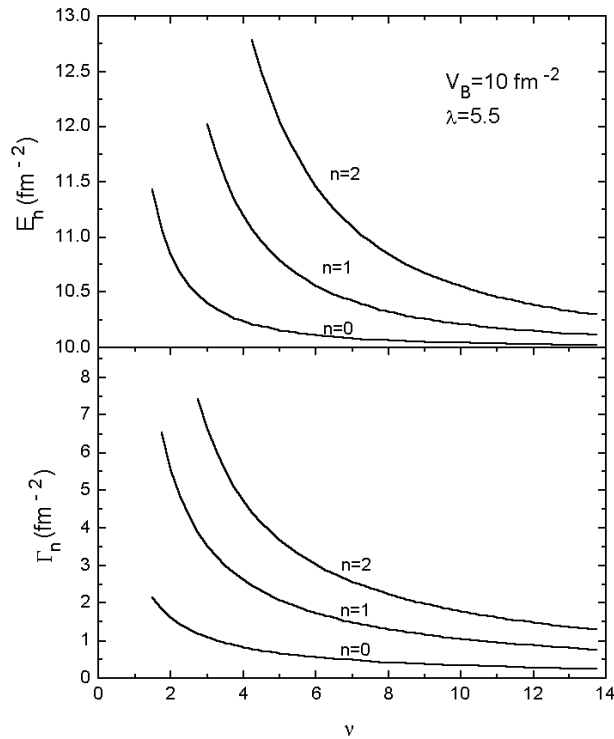


**Figure 2.** Upper panel: plot of resonance energy  $E_n$  as a function of range parameter  $\nu$ . Lower panel: plot of width  $\Gamma_n$  as a function of  $\nu$ . These results correspond to a barrier with  $\lambda = 5.5$  and a fixed height  $V_B = 10 \text{ fm}^{-2}$  at the origin.

only expect clear manifestation of the  $n$ th resonance without being blurred by the neighbouring resonances. In our case, we have from (20)

$$\Delta E_n = E_{n+1} - E_n = 2V_0(\lambda^2 - 2)(n + 1). \quad (31)$$

We search for the values of the barrier parameters  $\lambda$  and  $\nu$  which give the result  $\frac{\Delta E_n}{\Gamma_n} \geq 1$  and exhibit their manifestation in the results of transmission coefficient  $T_c$  given by equation (19). In figure 3, we plot first the ratio  $\frac{\Delta E_n}{\Gamma_n}$  as a function of the range parameter  $\nu$  for a fixed value for flatness  $\lambda = 5.5$  and height  $V_B = 10 \text{ fm}^{-2}$ . We see that the condition  $\frac{\Delta E_n}{\Gamma_n} \geq 1$  is satisfied by smaller values of  $\nu$ . Looking at figure 3, we consider two values of  $\nu$  with reference to the  $n = 0$  state, (i)  $\nu = 3$  such that  $\frac{\Delta E_n}{\Gamma_n} \geq 1$  and (ii)  $\nu = 5$  such that  $\frac{\Delta E_n}{\Gamma_n} < 1$ , and plot the values of  $T_c$  (19) as a function of  $E$  in figure 4, where  $\lambda = 5.5$  and  $V_B = 10 \text{ fm}^{-2}$ . The solid curve, representing results with  $\nu = 3$  satisfying  $\frac{\Delta E_n}{\Gamma_n} \geq 1$ , shows resonance peaks distinctly. On the other hand, the dotted curve, corresponding to  $\nu = 5$  satisfying  $\frac{\Delta E_n}{\Gamma_n} < 1$ , does not manifest the resonances clearly.

However, we have seen earlier that a larger value of  $\nu$  makes the barrier long ranged and generates resonances situated close to the top of the barrier, and also these resonances are narrower. That is, sharper resonances are crowded near the top of the barrier for larger  $\nu$  with  $\lambda^2 > 2$ . However, as discussed above, in order to have a distinct manifestation, smaller values of  $\nu$  generating short-ranged barriers are preferable. Further, the number of distinct ABRs increases with the increase of the value of the parameter  $\lambda$ , generating a flatter barrier top.

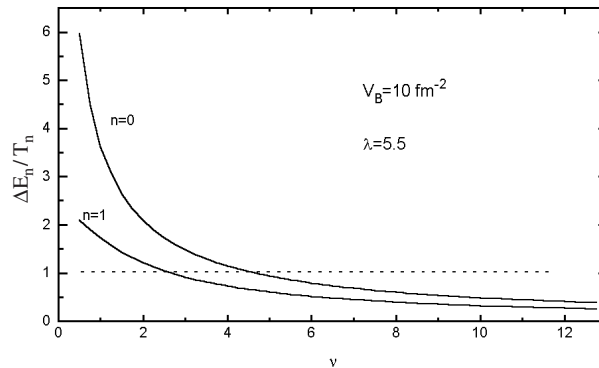


**Figure 3.** Plot of the ratio of energy level difference  $\Delta E_n$  given by (31) (see text) and width  $\Gamma_n$  given by (21) as a function of range parameter  $\nu$ . This corresponds to fixed barrier of height  $V_B = 10 \text{ fm}^{-2}$  and  $\lambda = 5.5$ .

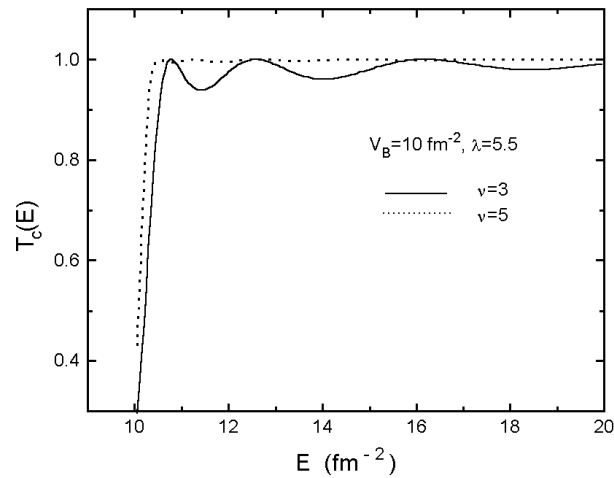


**Figure 4.** Plot of transmission coefficient  $T_c$  given by equation (19) (see the text) as a function of incident energy for the symmetric barrier of height  $V_B = 10 \text{ fm}^{-2}$  and flatness parameter  $\lambda = 5.5$ . The solid curve is for  $\nu = 3$  and the dotted curve for  $\nu = 5$ .

Thus, we have now a versatile exactly solvable potential which gives us a barrier that can be symmetric and asymmetric along with variable range and flatness at the top. This barrier can generate discrete ABRs with the condition that the flatness of the barrier represented by the parameter  $\lambda > \sqrt{2}$ . The analytical expressions for the transmission coefficient, resonance energy and width given in this paper can be of immense use in different branches of physics. In particular, one can use these results for better understanding of the orbiting-like phenomenon in the collision of two heavy nuclei. Further, some new features of fusion and molecular resonances in this collision process can be addressed. A preliminary calculation in this regard gives us encouraging results and this will be reported elsewhere soon.

## Acknowledgments

We are grateful to Professor L Satpathy for valuable discussion. BS acknowledges the support by BRNS, Mumbai vi-de research grant No 2000/37/11/BRNS/704.

## References

- [1] Newton R G 1966 *Scattering Theory of Waves and Particles* (New York: McGraw-Hill) ch 12
- [2] Cindro N 1981 *Riv. Nuovo Cimento* **4** 1
- [3] Ford K W and Wheeler J A 1959 *Ann. Phys., NY* **7** 259
- [4] Ford K W, Hill D L, Wakano M and Wheeler J A 1959 *Ann. Phys., NY* **7** 239
- [5] Child M S 1974 *Molecular Collision Theory* (New York: Academic)
- [6] Friedman W A and Goebel C J 1977 *Ann. Phys., NY* **104** 145
- [7] Brink D M 1985 *Semi-Classical Methods for Nucleus–Nucleus Scattering* (Cambridge: Cambridge University Press)
- [8] Rapp D 1971 *Quantum Mechanics* (New York: Holt, Rinehart and Winston) p 136
- [9] Ahmed Z 1991 *Phys. Lett. A* **157** 1
- [10] Ginocchio J N 1984 *Ann. Phys., NY* **152** 203
- [11] Ginocchio J N 1985 *Ann. Phys., NY* **159** 467
- [12] Ahmed Z 1997 *J. Phys. A: Math. Gen.* **30** 5243
- [13] Ahmed Z 1998 *J. Phys. A: Math. Gen.* **31** 3115
- [14] Sahu B and Shastry C S 1999 *J. Phys. G: Nucl. Part. Phys.* **25** 1909